Supplementary Information (ESI)

Anisotropic Atomistic Evolution During the Sublimation of Polar InAs Nanowires

Suji Choi,[a, b] Jeonghwan Lee,[a] Minwook Pin,[a, c] Ji-Hwan Kwon,[a] Min Sun Yeom,[d] In Kim,[d] Chung Soo Kim,[e] Ho Seong Lee,[b] Sang Jung Ahn,[a] Seong-Hoon Yi[b] and Young Heon Kim*[a,f]*

[a]Korea Research Institute of Standards and Science, 267 Gajeong-Ro, Yuseong-Gu, Daejeon 34113, Republic of Korea

[b]Department of Materials Science and Metallurgical Engineering, Kyungpook National University, Daegu 41566, Republic of Korea

[c]University of Science & Technology, 217 Gajeong-Ro, Yuseong-Gu, Daejeon 34113, Republic of Korea

[d]Center for Applied Scientific Computing, Korea Institute of Science and Technology Information, 245 Daehak-ro, Daejeon 34141, Republic of Korea

[e]Korea Institute of Ceramic Engineering and Technology, 101 Soho-ro, Jinju 52851, Republic of Korea

[f]GRAST, Chungnam National University, 99 Daehak-ro, Yuseong-gu, Daejeon 34134, Republic of Korea

KEYWORDS: In situ; polarity; anisotropic sublimation; surface energy; TEM

ESI 1:

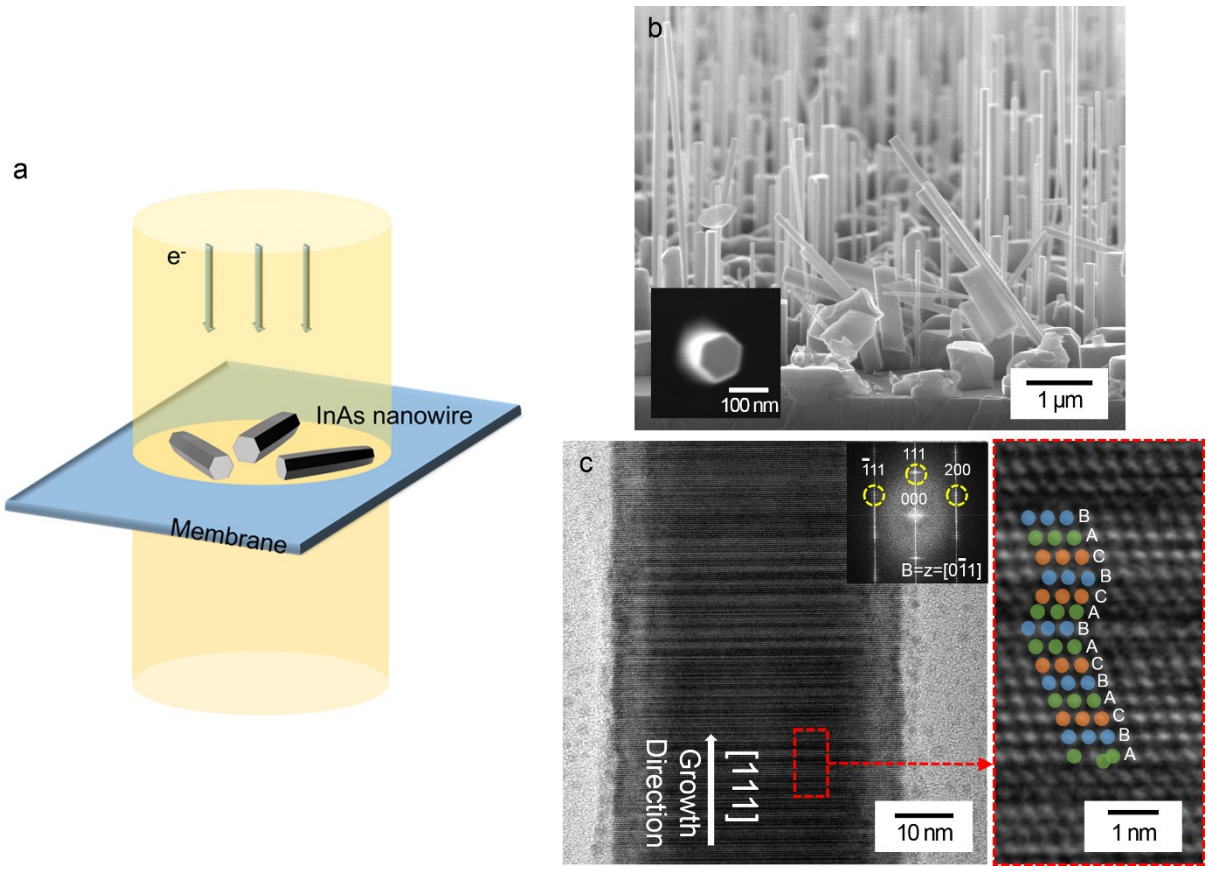

Fig. S1 (a) Schematic diagram of the heating experiment. (b) SEM image of the InAs NWs vertically grown on a Si(111) substrate. Top and cross-section images of InAs NWs. (c) HR-TEM image of InAs NWs. The stacking sequence represents the zinc-blende structure. There are many planar defects, stacking faults, and micro-twins.

Fig. S1a shows schematic diagram of the InAs nanowires (NWs) on the electronic heating chips (E-chips) and the electron beam. Fig. S1b shows cross- and top-view scanning electron microscope (SEM) images of InAs NWs. NWs grown on the Si(111) substrate with lengths in about 5 μm. As shown in the inset image of Fig. 1b, the cross-sectional geometry of the InAs NWs is hexagonal with diameters of 50–200 nm. The high-resolution transmission electron microscopy (HR-TEM) image shows representative microstructure of InAs NW, which is the zinc-blende structure, and the NWs have a uniform diameter of 50 nm, as shown in Fig. S1c.

The NW growth direction was determined to be the [] direction as shown in selected area electron diffraction (SAED) patterns. In the InAs NWs, stacking faults and micro twins was observed along the entire length of the nanowire. Therefore, strong streaks are shown in the SAED pattern (Fig. S1c inset). The measured lattice constant of the InAs nanowire of 0.35 nm is in good agreement with the *d*-spacing of the (111) planes of the InAs structure.

ESI 2: Decomposition at lower temperature

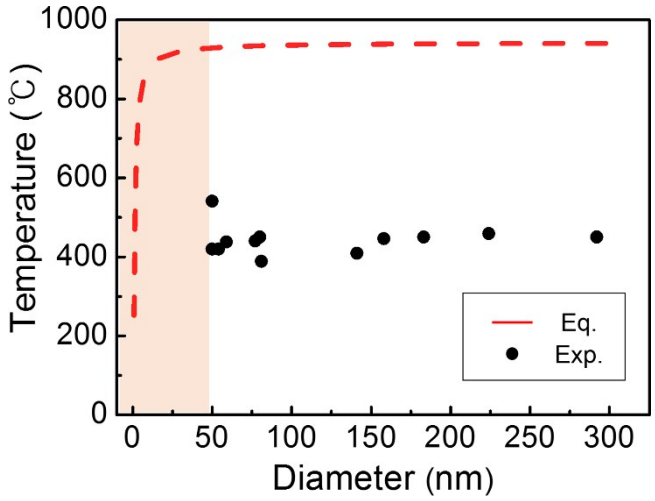

Fig. S2 (a) Schematic diagram of the heating experiment. (b) SEM image of the InAs NWs vertically grown on a Si(111) substrate. Top and cross-section images of InAs NWs. (c) HR-TEM image of InAs NWs. The stacking sequence represents the zinc-blende structure. There are many planar defects, stacking faults, and micro-twins.

The decomposition of InAs NWs started at around 380 °C during the continuous heating process. In addition, as shown in Fig. S2, the decomposition temperature is not dependent on the size of the InAs NW. The drop in the melting temperature of nanomaterials can also be explained by size effects.[1-3] Melting point depression has been described by the Gibbs–Thomson effect below the critical size of the nanomaterials in terms of the "classical thermodynamic model," "surface phonon instability model," and "liquid drop model." [1-3] The red dashed line in Fig. S2 shows the change in the melting temperature calculated using the classical thermodynamic model; the line clearly shows the drop of the melting temperature of the InAs NWs, particularly at 50 nm. However, there is a huge gap between the theoretical calculation used to explain the drop of melting points (red dashed line) and the experimental results (black square dots). Furthermore, the diameter of the InAs NWs treated in our experiment, 50–300 nm, is out of the size range for clearly showing the melting point drop,

that is, less than 50 nm. Therefore, we deduced that the decomposition of the InAs NWs at the low temperature observed in our *in situ* heating experiments was free from phenomena related to the size effect. In addition, the decomposition of the InAs NWs in our experiments did not result in the formation of alloys that could lower the melting temperature below the eutectic point because the NWs were composed of indium and arsenic alone and there was no growth catalyst. Furthermore, electron beam heating is one possible origin of the discrepancy between the red dashed line and the black squares. When the temperature rise induced by the electron beam was calculated using the equation formulated by Gryaznov et al.,[4] it was found to be approximately 40.0–85.5 °C under that generated under our experimental conditions, that is, an accelerating voltage of 300 kV and the electron current of 5.5 nA (see Fig. S3). However, we believe that the temperature increase induced by the electron beam is much lower that the calculated value because the boundary conditions are different from the assumptions used for the calculation; specifically, the geometry of a nanowire is quite different from that of the assumed nanosphere and the contact area with a supporting material is not a point as assumed in the equation. The InAs NWs were in contact with a relatively large area on the heating device. As demonstrated in our previous report, the NWs had a hexagonal shape in a cross section and were surrounded by the {220} surface plane. One of the {220} planes of the InAs NWs was in contact with the supporting material because these planes were aligned along the [110] direction of the zinc-blende structure. Although the NWs were heated by the electron beam during observation, the heat can be transferred to the surrounding materials easily. In addition, the temperature increase is small compared to the drop in temperature arising from decomposition, approximately 600 °C, even when heating by the electron beam was included. Therefore, we deduced that the heating by the electron beam had a negligible effect on the morphological and microstructural evolution. In contrast, the effect of the vacuum conditions during the heating was considered to be the principal origin of the low decomposition

temperature. In reality, the base pressure during the *in situ* heating experiment in TEM was approximately 10^{-7} Torr, that is, a high vacuum. The decomposition behavior is similar to the congruent vaporization of InAs reported by a few research groups. Shen et al. reported a congruent vaporization temperature of 353 °C considering the equal vaporization of In and As.[5] Other research groups have also reported congruent vaporization temperatures in the range of 370 to 390 °C.[6,7] Therefore, we concluded that the decomposition of the InAs NWs occurred via the congruent vaporization process under our experimental conditions.

ESI 3:

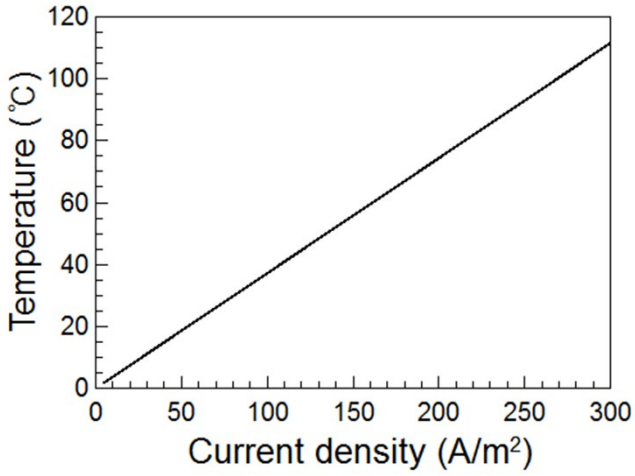

Fig. S3 Temperature increase versus current density arising from electron beam heating.

The electron beam used for the TEM analysis is one factor affecting the decomposition. As described in the main text, the accelerating voltage and the current of the electron beam for the TEM analysis were 300 kV and 5.55 nA, respectively. As demonstrated in our previous report, the InAs NWs experience direct atomic displacement and radiolysis during TEM observation. However, through the additional experiments, we found that the two effects had a negligible effect on the decomposition of the InAs NWs. In addition, electron beam heating is suspected to be the origin of the discrepancy between the red dashed line and the black squares. The current density in our experimental conditions was 110–230 A/m^2, and we used an average NW diameter of 105 nm for the calculation. The temperature generated by the electron beam ($\bar{T}$) is given by the following equation.[4]

$$\bar{T} = \frac{a^2}{6k}\bar{T}(\gamma) * \frac{\bar{\varepsilon}_b}{e}J$$

$$\bar{\varepsilon}_b = 2\pi r_e^2 ZN \frac{1}{E(2+E)mc^2}\left[(1+E)^2 \ln\left(\frac{E^2}{2I^2}(2+E)\right) - (1+2E)\ln 2 + 1 + \frac{E^2}{8}\right]$$

To calculate $\bar{T}$, it is necessary to calculate the electron energy loss per unit length, $\bar{\varepsilon}_b$, of InAs. Here, I is the mean ionization potential, E is the InAs ionization energy, N is the atomic density, and x is the sample thickness.

ESI 4:

Table 1 The defect formation energy at the surface *(hkl)*. Elements in subscript represent vacant atoms at the *(hkl)*-surface.

(hkl)	E_{defect} **(eV)**
111_{As}	-18.40
111_{In}	-2.02
211_{In}	-1.44
311_{In}	-1.10
100_{In}	0.24
$1\bar{1}1_{In}$	0.26
311_{As}	0.62
100_{As}	1.62
$1\bar{1}1_{As}$	3.19
211_{As}	3.62
110_{In}	4.47
110_{As}	5.89

Reference

1. N. Goldstein, C. M. Echer, P. Alivisatos, *Science*, 1992, **256**, 1425–1427.

2. M. Wautelet, *J. Phys. D. Appl. Phys.* 1991, **24**, 343.

3. K.K. Nanda, S. N. Sahu, S. N. Behera, *Phys. Rev. A*, 2002, **66**, 132081–132088.

4. V. G. Gryaznov, A. M. Kaprelov, A. Belov, *Philosophical Magazine Letters*, 1991, **63**, 275–279.

5. J. Shen, C. Chatillon, *J. Cryst. Growth*, 1990, **106**, 543-552.

6. C. E. C. Wood, K. Singer, T. Ohashi, L. R. Dawson, A. J. Noreika, *J. Appl. Phys.*, 1983, **54**, 2732–2737.

7. B. T. Meggitt, E. H. C. Parker, R. M. King, *Appl. Phys. Lett.*, 1978, **33**, 528.